Received September 11, 2015, accepted September 28, 2015, date of publication October 7, 2015, date of current version October 14, 2015.

Digital Object Identifier 10.1109/ACCESS.2015.2487859

Algorithms for Size and Color Detection of Smartphone Images of Chronic Wounds for Healthcare Applications

TIK WAI (KIRAL) POON[1] AND MARCIA R. FRIESEN[2]
[1]Department of Computer Science, University of Manitoba, Winnipeg, MB R3T 2N2, Canada
[2]Department of Electrical and Computer Engineering, University of Manitoba, Winnipeg, MB R3T 2N2, Canada

Corresponding author: M. R. Friesen (marcia.friesen@umanitoba.ca)

This work was supported by the Natural Sciences and Engineering Research Council of Canada.

ABSTRACT A mobile app for smartphones and tablets to document pressure ulcers was previously developed. The mobile app is part of the rapidly growing field of mobile health. The mobile app replaces paper-based documentation in a healthcare facility with an electronic record. In a user trial in 2013, a key finding was the high value attributed to wound image (photograph) galleries in the mobile app and wound tracking though graphing progression. Consequently, work was undertaken to enhance the imaging features by developing image analysis algorithms for size and color determination of wounds from wound images taken with an on-board smartphone or tablet camera, using no peripheral hardware or ancillary devices in setting up the image. The reliance solely on the internal smartphone sensors to generate high-accuracy measurements brings novelty to the work and specifically in the field of wound management. The work includes three components. The first component, referred to as mask image, obtains the dimensions of an object in the image. The second component, referred to as camera calibration, reconstructs an image taken on an angle (3-D) referenced back to a 2-D plane. The third algorithm determines the range of colors present in an image, separating the image into three component colors by extracting components from the Red Green Blue format of the image, and converting output to red yellow black. An expert system and/or machine learning is recommended to enhance the correlation of wound color to wound stage.

INDEX TERMS Algorithms, image analysis, smartphones, wound care.

I. INTRODUCTION & OBJECTIVE

The research group previously developed a mobile app called SmartWoundCare for Android and iOS smartphones and tablets to document and assess chronic wounds, specifically pressure ulcers (bedsores) [1]. The mobile app is part of the rapidly growing field of mobile health or mHealth, or the delivery of healthcare and healthcare support through mobile devices. Mobile consumer devices are increasingly capable of meaningful applications in mHealth, and examples range from apps that allow users to track diet and fitness, health condition monitoring (e.g. diabetes [2]; arthritis [3]), and the use of mobile devices to replace paper records and share information between healthcare providers (see [4]).

This paper outlines the application of mobile consumer devices to automated wound analysis and classification. Specifically, work was undertaken to develop algorithms to generate wound size and to analyze wound color from a wound image taken by a smartphone or tablet camera, without the use of peripheral or auxiliary devices such as positioning templates, ultrasonic transducers, or additional lenses. This is in contrast to work by others which, for example, controls lighting and wound position with an image capture box when performing image analysis of diabetic foot ulcers [5]. The reliance on the internal smartphone sensors alone to generate high-accuracy measurements brings novelty to the work and specifically to the field of wound management.

II. BACKGROUND

A. PRESSURE ULCERS AS THE FOCUS AREA

Pressure ulcers, also known as bedsores or decubitus ulcers, were chosen as the focus area for the mHealth app due to their significant prevalence and associated impacts in healthcare. Pressure ulcers most commonly affect persons with limited mobility and the elderly. The negative impacts of pressure ulcers include impacts on patients' recovery from other conditions, mobility, social isolation and quality of life factors, secondary infections, and mortality. Concomitantly, there is an increasing emphasis on electronic communication

in pressure ulcer management to improve the efficiency of care, the patient and caregiver experience, and ultimately the clinical outcomes. EHealth and mHealth initiatives in wound care are conjectured to assist in pressure ulcer prevention and treatment by facilitating different types of healthcare interventions, changing user behaviors, enhancing communication between patients and providers, and providing education [6]–[9].

B. PRIOR WORK IN THE RESEARCH GROUP: SMARTWOUNDCARE

SmartWoundCare, an existing mobile app for wound documentation developed in the research group, replaces the patient's paper-based chart in a hospital or personal care home with an electronic record [1]. SmartWoundCare was developed to improve patient/caregiver communication as well as communication between multiple healthcare providers, facilitate patient engagement in their own care, and improve wound management and outcomes. In addition to replicating the paper-based chart, SmartWoundCare also offers alerts/alarms for user-set conditions, automatically generates wound histories in text, graph, and image (photos) formats, and is positioned for telehealth.

SmartWoundCare was trialed at a personal care home in Winnipeg, Canada in summer 2013. A key finding of this user trial was the high value attributed to wound images (photographs) [6]. The value of the photographs extended to the patient, the patient's family, and the healthcare providers. The benefits included the ability to show patients wounds that they could not otherwise see (e.g. wounds on buttocks, back of legs, or under the foot), patients' and families' enhanced understanding of the wounds and subsequent compliance with wound care directives, consultation with other healthcare providers with a wound photograph which then saved time otherwise needed to undress and redress a wound, and the value of the image in augmenting the written chart as part of the overall patient record.

This finding is congruent with others' findings on the value of wound photography in other types of chronic wounds. Two separate studies compared the measurement accuracy of venous leg ulcers and diabetic foot ulcers, respectively, made via traditional measurement techniques vs. measurements taken from digital images [10], [11]. Traditional methods of wound measurement are to trace the margin of a wound on transparent film, and then overlay the transparent film on to graph paper and count the number of squares. Comparing this method to measurements of tracings taken from digital images, researchers reported better accuracy, less inter-observer variations in measurements, and better ease of use with the computer-aided method. As a non-contact method, the researchers also reported an improved patient experience. In another study examining the outcomes of pressure ulcer assessment done via videoconferencing relative to in-person assessment, researchers found very strong agreement in the staging of the wound between the two approaches, but the assessment of wound volume to be somewhat larger when assessed via videoconference than when assessed in person [12]. In general, these findings are consistent with research that highlights the value of visual information in mHealth to user engagement and compliance [3].

Given the finding of the high value of wound photographs, initial work was undertaken to develop algorithms that would add intelligence to the SmartWoundCare app by automatically generating the wound size from the image. In this way, a chronology of wound size would provide information on wound status and healing. The objective was scoped such that the image analysis algorithm(s) would facilitate non-contact measurements of irregularly-shaped images taken with a sole smartphone or tablet camera, using only the sensors integrated in the smartphone or tablet with no auxiliary or add-on instrumentation on the device, and where the measurements have less than 10% error, for images taken from distances of up to 30 centimeters. Initial research explored one method for determining distance to the wound (camera to wound) and two algorithms to determine wound size. Although both showed promise, the specifications for error were not met [7].

The objective of the current work was to develop algorithms that auto-generate wound size (relative and absolute) and an analysis of wound color, without the use of peripheral devices on the smartphone or tablet to either record or manipulate the image. In downstream use, the development of a wound image library generated by a collection of images generated by the community of users of the app would allow for potential Big Data applications, such as mining and analyzing the data to develop predictive inferences that can eventually feed into the body of knowledge for wound treatment and prevention.

C. IMAGE ANALYSIS FROM PHOTOGRAPHY

Although smartphone and tablet cameras are universally used for recreational photo capture and sharing, the built-in cameras are not generally used for applications that require high accuracy, precision, and resolution. This is changing rapidly, with each new smartphone release boasting higher-resolution cameras.

Our prior work reviewed the current state of image analysis from photography [7]. In that publication, an overview was provided for mobile apps for Android and iOS for mid-range object measurement applications (generally 0.5m to 20m) [13], [14], ultrasonic-transducer rangers [15] for objects at shorter distances (1cm – 6m), infrared distance measuring [16] to measure shorter distance (4cm – 30cm) and laser rangers. Outside of the smartphone / tablet domain, depth-of-field cameras were also reviewed [17]–[19].

At time of writing, it is anticipated that smartphones with integrated dual-lens cameras are poised for mass market entry in the foreseeable future [20]. This would add inherent capability of offering enhanced, accurate and high precision imaging amenable to follow-on analysis and characterization, building on the technology expertise and applications of stereoscopic cameras in other fields such as manufacturing.

Google's Project ARA, a collaborative effort to develop modular smartphone hardware may also provide a future framework by which to include dual-lens cameras in mobile devices.

III. IMAGE ANALYSIS

Algorithms were developed to determine the dimensions of irregularly shaped images – in this case, wounds on skin – and to determine the color breakdown of the wound. The algorithms used data generated solely by the sensors integrated on a smartphone, without the use of peripheral or add-on devices or auxiliary devices such as positioning templates or ultrasonic transducers. The reliance solely on internal smartphone sensors to generate high-accuracy measurements brings novelty to the work, and specifically to the field of wound management.

Three components of the work are outlined below. In the first component referred to as Mask Image, the objective is to obtain the comparative dimensions of an object in the image. The second component, referred to as Camera Calibration, reconstructs an image taken on an angle (3D) referenced back to a 2D plane. The third algorithm determines the range of colors present in an image, separating the image into three component colors by extracting components from the RGB format of the image.

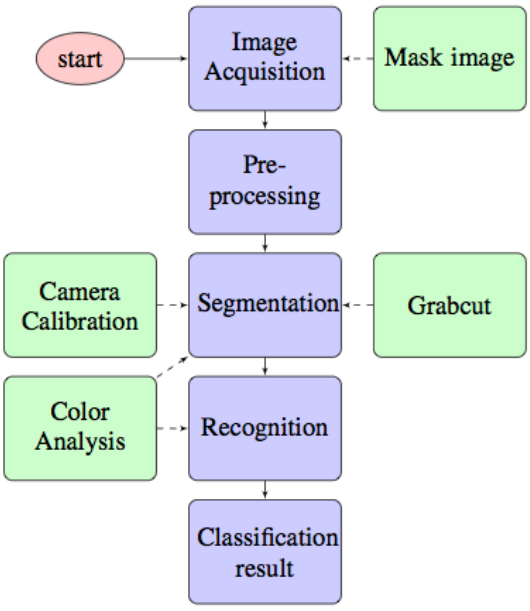

FIGURE 1. Basic Application Model.

The application model consists of different modules including wound image acquisition, wound image preprocessing, image segmentation, wound type recognition, and classification. Figure 1 provides a top-level view of this sequence. The Mask Image component is within the image acquisition stage. Grabcut as a segmentation method [21] and the Camera Calibration component are both a part of the segmentation phase. The color analysis module is a part of the segmentation and recognition phases.

All wound images are taken by smartphone on-board cameras or by webcam as specified below. All images are currently processed on a computer rather than on the smartphone itself. This enhances the robustness for the user, who is able to select a webcam for use in a static environment like a hospital or home, or to use the smartphone camera. This work supports both of the cases with their associated benefits and liabilities.

A static environment includes a fixed camera setup and a fixed wound position, and generally a more stable light source. The Camera Calibration module only needs to be done once on a plane. A dynamic environment denotes a mobile camera (i.e. smartphone or tablet) and the patient in a natural position without props or staging devices. Mask image acquisition is needed, and the Camera Calibration module will need to be carried out repeatedly if the actual size of objects (as opposed to relative size) is needed.

For this work, the following hardware and software specifications were used (Table I), and computation times were measured in seconds, rather than minutes or hours.

TABLE 1. Hardware and software specifications.

Nexus 4 (LG-E960)
Krait Quad-core 1.5GHz
Display resolution 1280x768
Camera resolution 8MP (3264x2448)
High Performance Adreno 320 GPU
Bluetooth 3.0 BLE
Wi-Fi 802.11 a/b/g/n
Samsung Galaxy S4
ARM Cortex-A15 Quad-core 1.9 GHz processor
Display resolution 1080 x 1920
13+ megapixel camera
Bluetooth 4.0
802.11 a/b/g/n
Samsung Galaxy S4
MacBook Pro
Processor 2.6 GHz Intel Core i7
Memory 8 GB 1600 MHz DDR3
Graphics Intel Iris Pro 1024 MB
Software OS X 10.9.5 (13F34)
Software
Android 4.2 (Jelly Bean)
Android NDK r9d
OpenCV 2.4.9 Android SDK
Python 2.7.10
Numpy
Matplotlib
OpenCV 3.0.0
Matlab

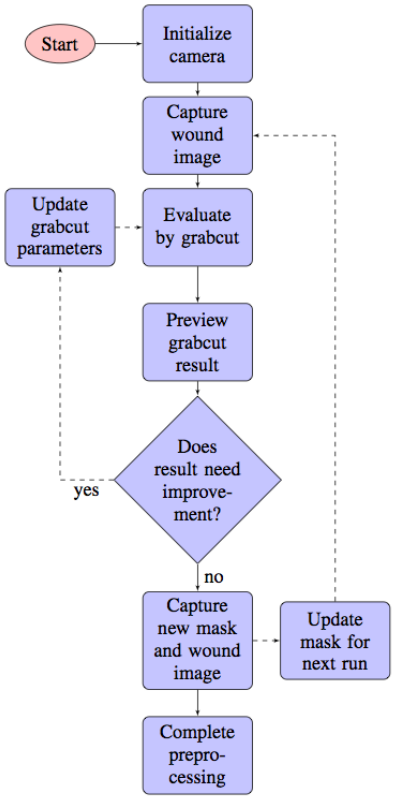

FIGURE 2. Image acquisition and pre-processing flow chart.

A. MASK IMAGE

Figure 2 provides an overview of the first two segments of the basic application model (Fig. 1), which includes the Mask Image component.

The Mask Image and the Camera Calibration components focus on determining the relative and absolute size of the wound. Currently, the most common way to measure wound size is to apply a disposable adhesive measuring tape alongside the wound, and by using a marked cotton-tipped applicator to measure depth. By convention, wound length is measured in the head to foot direction at the point of maximum length; and the width is from one side of the wound to the other side of the wound at the point of maximum distance. Undermining refers to a wound that is larger in area at its base than at the skin surface. It is a wound which essentially is a larger cavity beneath a smaller opening at the skin surface. A cotton-tipped applicator is used to measure the deepest point of the wound, from the surface of the wound to tip of the applicator at the deepest part of the wound. In some cases, undermining will be recorded according to a clock face, where the head will be 12 o'clock and the foot will be 6 o'clock.

Two existing approaches to automatically generate wound size include grid capture and scanner capture. In the grid capture approach, a transparent double layer film with a marked grid (1×1cm) is placed on the wound and the wound contour is traced with a black permanent marker [5], upon which the length and the width can be easily calculated by a smartphone application. The area of the wound can be calculated by the factor between the grid and the pixel. The advantage of this method is that the transparent film is placed directly on the wound, keeping the traced wound at the near dimension and orientation as the real wound underneath, minimizing distortion or uncertainty of the wound image area.

In the existing scanner capture approach, a box with two mirrors inside is placed at 45 degrees relative to the horizontal, with openings for a smartphone and an LED light source [22] and this configuration acts as a scanner to scan the wound. The configuration ensures a constant light source location and intensity, and a constant known distance is maintained between the camera and the wound, facilitating area calculations. The image capture box will keep a constant distance and will be known, hence the ratio of the size of the wound image will be also constant. This method again relies on auxiliary devices (the box and mirror) and will be cumbersome or impractical for wounds on certain parts of the body. As a contact-based design, this method may have less utility when serving as a measurement procedure for a large number of patients.

In our previous work, a ''pinch-zoom'' method of wound size calculation was developed, using the device itself as a reference and comparing it side by side with the object image to achieve the size via the ratio [7]. The method has high mobility; however, accuracy is somewhat user-dependent and not systematic. The same person doing the same size estimation with the new image may generate variable results.

In the current work, the first component is referred to as Mask Image, where the objective is to obtain the comparative dimensions (change in dimension) of an object in the image relative to a previous image of the same wound. The user aligns a transparent mask overlay of the wound from a previous assessment on the wound during the current assessment. The algorithm compares the previous image to the subsequent or new image by recognizing and aligning wound perimeters where they have stayed constant and then estimates the relative size difference in order to infer healing or deterioration (Fig. 3 and 4). The result is given as a percentage change in

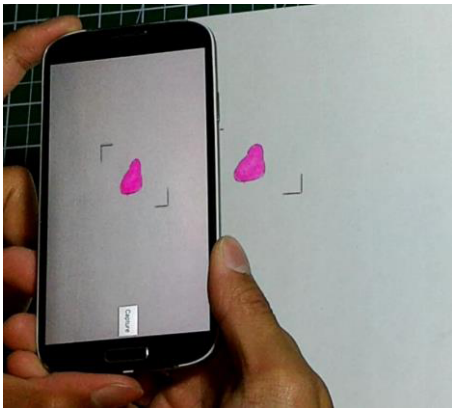

FIGURE 3. Creating a mask image from the wound.

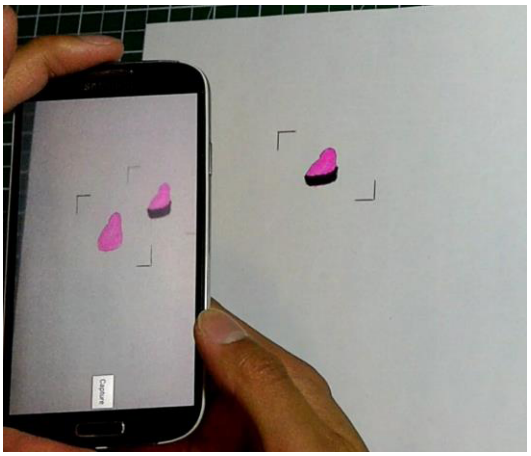

FIGURE 4. Overlap of mask image to a new wound.

the area of the most current image relative to the Mask Image. If the real-world size of the wound is needed, then the pinch-zoom method [7] and camera-calibration method discussed in the subsequent section can be applied.

The transparent mask overlay does not need to be limited to the wound image; for example, a medical tattoo can act as a reference point for the Mask Image as well. A medical tattoo is either a temporary or permanent tattoo or skin marker, used to ensure targeted consistency in medical therapy or treatment – in this case, the alignment of a camera relative to a wound. For example, a tattoo of three dots or lines around the wound can serve as a pattern to ensure alignment of successive mask images. Invisible tattoos are also possible, although they then require a peripheral device with UV light during image capture.

The outcome is a relative dimension of the image (previous assessment to current assessment) which leads to a better estimation of whether the wound is healing. The error inherent in this method is largely associated with the user, including the sharpness of the mask and the user's skill in aligning the mask over the current wound. During image acquisition, the image consistency should be maintained as high as possible for image clarity and subsequent dimensional comparisons and inferences of healing or deterioration. The depth of the wound is also an important parameter to compare the status of the wound from one assessment to the next. In the current standard of smartphone cameras, it is not readily possible to generate the depth of an image. Hence, instead of adding an external device to potentially infer depth in an image, an analysis of the wound color will help determine the stage of the wound.

The advantage of the Mask Image approach over existing approaches is that no peripheral devices to the smartphone camera or staging props are required. One does not need a ruler on the body part, as the outcome is the relative size of the wound from one assessment to another, rather than the actual size in the real world. When the algorithm is implemented with a Camera Calibration component, an absolute dimension is possible. However, the efficacy of the approach may depend on the skin tone and how well the surrounding skin is differentiated from the wound. In this case, a medical tattoo may be used as the Mask Image.

B. CAMERA CALIBRATION

Figure 5 shows the Camera Calibration module within the overall process outlined in Fig. 1.

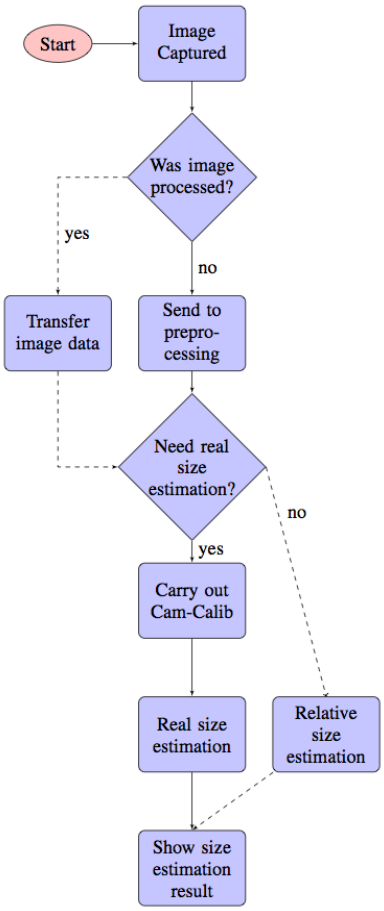

FIGURE 5. Size estimation with segmentation flow chart.

The grabcut algorithm plays an important role in this application, as a segmentation method by which to isolate the wound from the background, producing what is referred to here as a segmented image. This segmented image is further used in the Camera Calibration module and the color analysis module. Compared with other algorithms, grabcut provides efficient results with minimal human interaction [21], and this is its key benefit in the current work. A user is able to identify and label the foreground and the background object through the tool using the grabcut segmentation method (Fig. 6). In this application, the foreground is the wound and the background is the surrounding skin or body part and surroundings.

To estimate size, the segmentation method compares pixels of two images, which assumes that the dimension of the image captured is close to the previous image. The algorithm then calculates the relative change in size between the

FIGURE 6. Grabcut applied as a segmentation method.

two images. If an actual dimension is needed, then this segmented result is sent to the Camera Calibration component. A demonstration of the grabcut algorithm applied to wound care is available at https://youtu.be/Iyvochswrws.

The Camera Calibration module reconstructs an image taken on an angle (3D) and references it back to a 2D plane. The algorithm uses a designated pattern with at least 13 known reference points and applies the Tsai2D algorithm [23], [24] to obtain a reconstructed image of the wound. Since the distance between the points are known from the calibration model, the view angle can be calculated and the image can be reconstructed on a 2D plane. The outcome is a reconstructed 2D image and the size of the wound can be calculated from that 2D image. This method can be partnered with the Mask Image method to get the actual size of the wound. This algorithm cannot identify depth nor volume of wounds with significant undermining.

In this work, a chess board pattern was used in the Camera Calibration module, which worked effectively in both the static and dynamic environments. In traditional wound measurement, a paper ruler would be placed near the wound to determine size, with the assumption that the wound is in a 2D plane, and that the wound and the ruler are in the same 2D plane. In this work, the chess board pattern is placed close to the wound in order to obtain the size of the wound on the same plane as a ruler, and where the planar orientation of the chess board pattern was also able to be calculated and corrected. This method adopted from Baltes & Anderson's work [25], in which Camera Calibration was used to achieve the dimension of a soccer field, reconstructed in a top view based on extrinsic parameters achieved after the Camera Calibration. In the current application, the sticker will be the calibration pattern to obtain the extrinsic matrix of the wound, allowing for systematic size estimation (Fig. 9). The extrinsic matrix describes the camera's location and view direction, including a rotation matrix and a translation matrix. Extrinsic values can be generated, for example, formed by Fig. 7a or 7b, provided the chess board pattern exists.

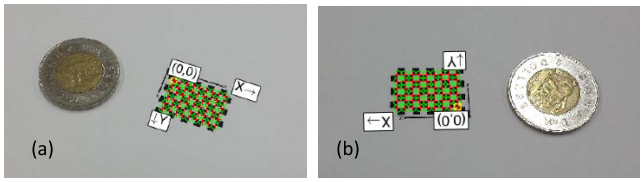

FIGURE 7. a & b Detected image points and re-projected points in two different planes.

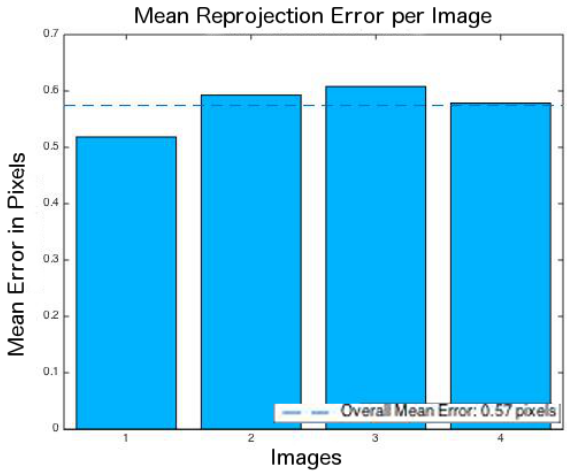

FIGURE 8. Mean re-projection error per image.

```
Intrinsics
----------
Focal length (pixels):   [ 7232.2731 +/- 627.2535   4201.5799 +/- 621.9988]
Principal point (pixels):[ 2258.3928 +/- 142.9575 -4609.8744 +/- 1787.3598]
Radial distortion:       [   -0.0563 +/- 0.0197        0.0036 +/- 0.0038  ]

Extrinsics
----------
Rotation vectors:
                         [   -1.1583 +/- 0.2545       -0.0749 +/- 0.0331        0.4338 +/- 0.0497  ]
                         [   -1.0548 +/- 0.2532        0.6291 +/- 0.1645        1.5247 +/- 0.0290  ]
                         [   -0.1237 +/- 0.0445        1.2961 +/- 0.2380        2.1475 +/- 0.1766  ]
                         [    0.2216 +/- 0.0974        1.4309 +/- 0.2661        2.6588 +/- 0.2220  ]

Translation vectors (mm):
                         [ -127.6825 +/- 65.5766   4830.3565 +/- 2298.9519   2991.6657 +/- 382.3399]
                         [  -26.1324 +/- 68.0065   4926.9088 +/- 2335.7313   3028.4934 +/- 390.2224]
                         [   26.9854 +/- 67.7615   5011.7455 +/- 2331.8382   2959.1289 +/- 400.8007]
                         [   16.9656 +/- 69.0553   5131.9501 +/- 2379.4611   3019.0809 +/- 411.7043]
Measured diameter of one loonie as Wound = 300.61 mm
```

FIGURE 9. Extrinsic parameters from camera calibration.

Although the Mask Image method and the Camera Calibration method serve different purposes in the application, they both increase the applicability of the application and allow more systematic size estimates. Using these methods, the actual size of a dollar coin was estimated with an error of <1% (Figs. 7-9). Figures 7a and 7b demonstrate that the algorithm can be applied at various angles, rather than only at the perpendicular to the object being measured.

Figures 10-12 demonstrate the original and re-projected planes (red vs. green lines), applied to the reconstruction of a wound in the Camera Calibration module. The red lines represent the detected objects (block). The algorithm grabs the centre of each object and sends the image coordinates to be processed via the Tsai2D algorithm. The blue color lines denote the scanning sequence. Because the pattern size is fixed and known, the algorithm can generate model coordinates of each block, which can be converted back to image coordinates to confirm the result. In Fig. 10, the green lines are the re-projected lines from the model points to the real world coordinates, which show how effective the camera calibration method was. Curved or other irregularly shaped green lines would indicate a problem with the re-projection. In application, a wound photographed on an angle (Fig. 11) is reconstructed and re-projected on a plane perpendicular to the viewer (Fig. 12).

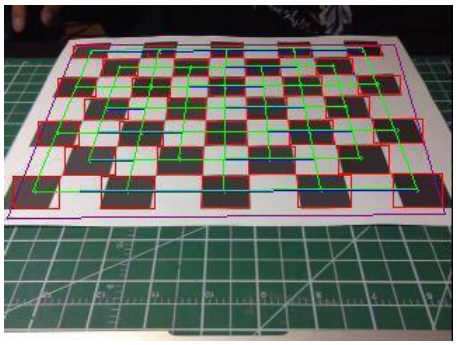

FIGURE 10. Original and re-projected planes.

FIGURE 11. Wound image before reconstruction.

FIGURE 12. Wound image after reconstruction.

A demonstration of the Camera Calibration module is available at https://youtu.be/OiJk3nMymSE.

C. COLOR ANALYSIS

The third algorithm determines the range of colors present in an image, separating the image into three component colors by extracting components from the RGB format of the image and presenting them in a histogram. Each component has a defined range, and a template palette can calibrate the colors under different lighting conditions. These data can then serve as input into a determination of the stage the wound. Figure 13 shows the Color Analysis module within the overall process outlined in Fig. 1.

Pressure ulcers fall into six potential stages (stage I through IV, Suspected Deep Tissue Injury, and Unstageable) [26]. Due to the limitation of our work in assessing depth of wounds, the last two categories are combined into a single Unstageable category. Parameters that determine wound staging include whether the skin is intact

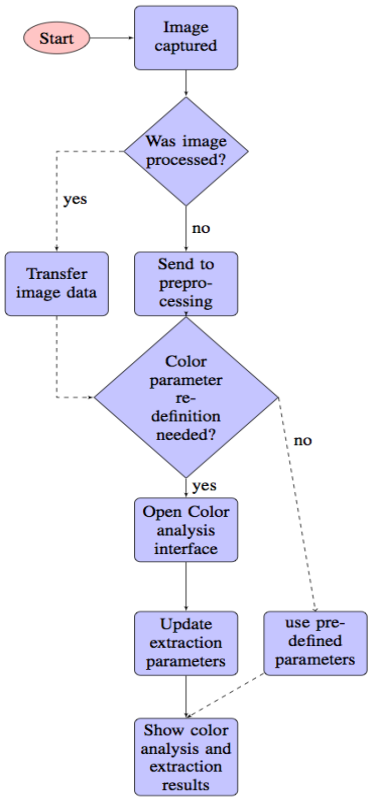

FIGURE 13. Color analysis flow chart.

or broken, tissue loss, skin, tissue, and wound bed color, and the presence of slough and eschar.

The algorithm separates the image into three component colors by extracting components from the RGB format of the image. Each component has a defined range, and a template palette can calibrate the color under different lighting conditions. To avoid lighting problems, natural light and the use of camera flash is recommended, to maintain the consistency of the light. However, the user can also re-define the color parameters through an interface when required for different lighting in different environments.

Color analysis greatly improves after segmentation is carried out (Fig. 14 and 15). After segmentation with the grabcut algorithm, the background noise has been cleared and the user interface shows the model colors properly. Although the RGB format is used in this application, the Hue, Saturation, Value (HSV) format is also a good option because it responds to lighting and may be more amenable to tuning color. The images used here were acquired from http://reference.medscape.com/features/slideshow/pressure-ulcers.

The RGB results can also be converted to RYB (red yellow black) ratios, which have a more direct relationship to wound classifications. Further, Figure 16 demonstrates a preliminary classification of RYB output to wound stage. Wound stages I and II are differentiated by the intensity of red, while wound stages III through V rely on relative prevalence of red, yellow, and black in the image.

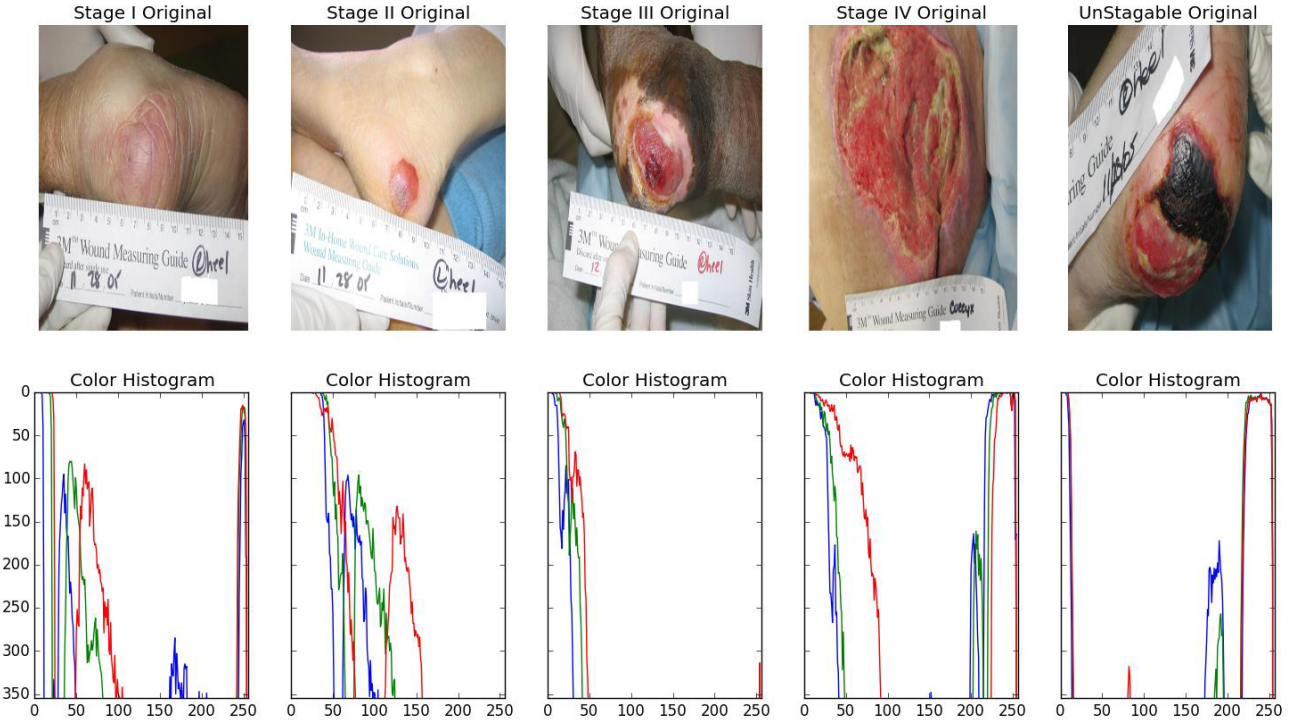

FIGURE 14. Histogram results on different stages before segmentation.

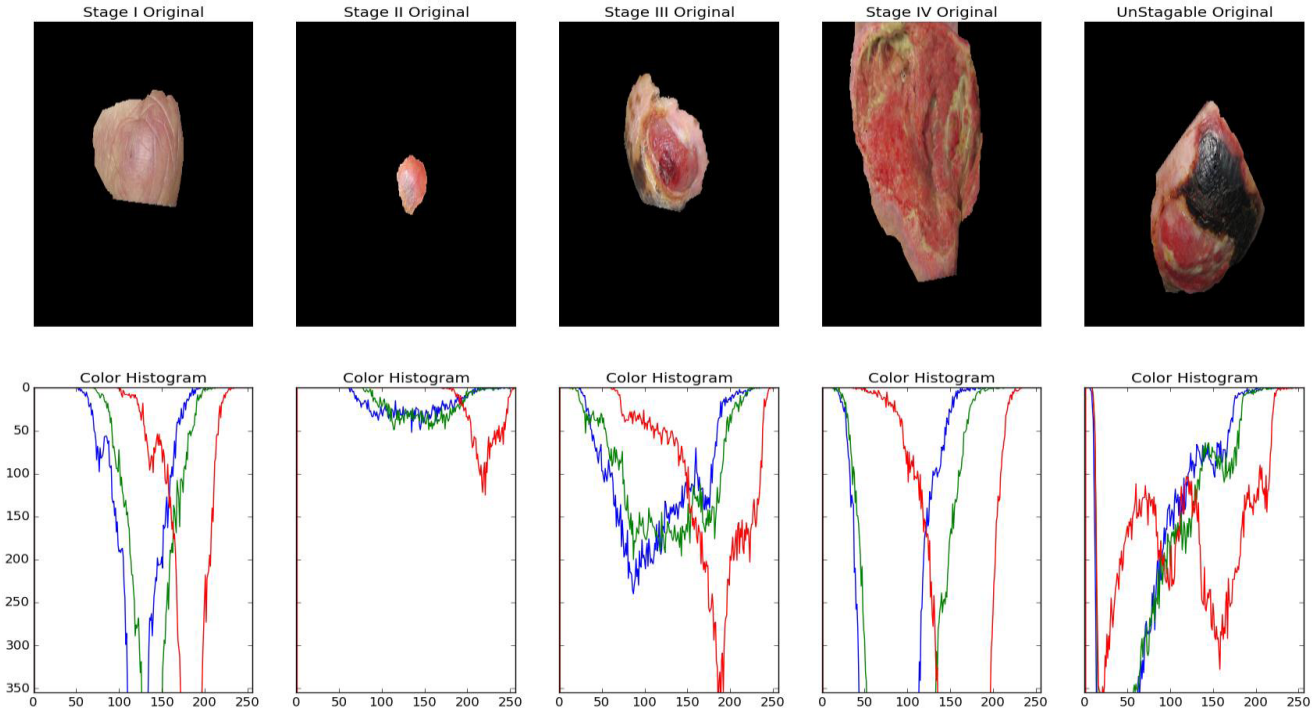

FIGURE 15. Histogram results on wounds of different stages after segmentation.

The error inherent in this method depends to some extent on the definitions of colors that the user sets, and therefore it is recommended to use a large data set to define the parameters and to partner this module with machine learning.

After the color is extracted, results can be sent to an expert system to determine the wound stage. Currently, the expert system framework has been developed, but has not been populated with training data. As such, the work here was

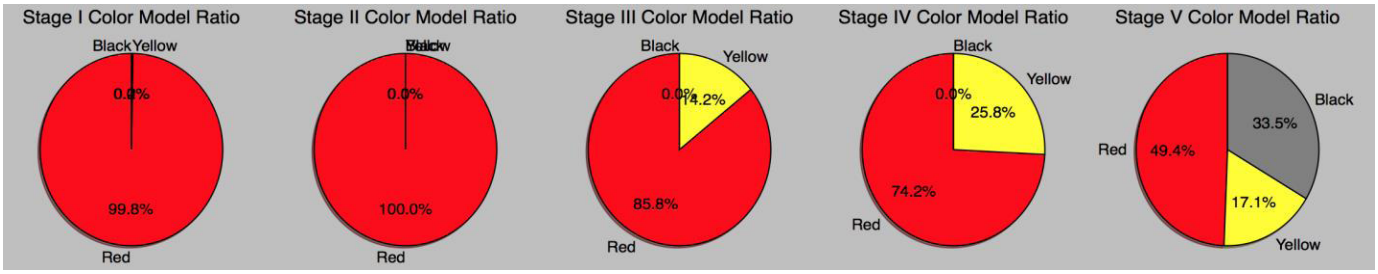

FIGURE 16. RYB output correlated to wound stage.

limited to the development of the algorithms to extract and present color components. Systematically evaluating wound staging based on a statistically significant set of wound images, and then comparing the results to traditional methods of wound classification by manual inspection by a practitioner are future work. As an alternative to an expert system, results could be fed to a machine learning algorithm like SVM (Support Vector Machine) or decision tree to help determine the wound stage.

A demonstration of the color analysis module is available at https://youtu.be/Iyvochswrws.

IV. CONCLUSION

This paper has presented a prototype to automate chronic wound analysis and classification using readily-available consumer mobile devices, specifically smartphones and tablets. Previous work resulted in a mobile app for electronic documentation of chronic wound management. This work focussed on maximizing the value of wound images generated within the mobile app. Algorithms were developed to automatically detect size of wounds both relative to previous assessments and real-world size, as well as an analysis of color(s) present in a wound in order to ultimately correlate color to wound stage.

Future work will focus on the training of an expert system and the development of machine learning elements to determine the wound stage, based on the outputs of the other modules which determine size and color of the wound.

The algorithms developed in this work are not limited to pressure ulcers but can also be applied to other wounds, moles, or other objects on patients. The analysis and extraction of color can be also applied on other kind of medical images to feed expert systems or machine learning algorithms. In mobile healthcare apps, there is a growing awareness of the ability to crowdsource data (in this case, images) from other app users which can increase the robustness of expert systems.

REFERENCES

[1] J. Vivanco, J. Haydaman, C. Hamel, R. D. McLeod, and M. R. Friesen, "Development of wound care software for smartphones and tablets," *Wounds Int.*, vol. 3, no. 3, pp. 13–14, 2012.

[2] J. A. Cafazzo, M. Casselman, N. Hamming, D. K. Katzman, and M. R. Palmert, "Design of an mHealth app for the self-management of adolescent type 1 diabetes: A pilot study," *J. Med. Internet Res.*, vol. 14, no. 3, p. e70, 2012.

[3] *Georgia Tech GVU Centre: RheumMate*. [Online]. Available: http://gvu.gatech.edu/research/projects/rheummate, accessed Jun. 10, 2015.

[4] *Health Outcomes Worldwide*. [Online]. Available: http://healthoutcomesww.com, accessed Jun. 10, 2015.

[5] L. Wang, P. C. Pedersen, D. M. Strong, B. Tulu, E. Agu, and R. Ignotz, "Smartphone-based wound assessment system for patients with diabetes," *IEEE Trans. Biomed. Eng.*, vol. 62, no. 2, pp. 477–488, Feb. 2015.

[6] M. R. Friesen, C. Hamel, and R. D. McLeod, "A mHealth application for chronic wound care: Findings of a user trial," *Int. J. Environ. Res. Public Health*, vol. 10, no. 11, pp. 6199–6214, 2013.

[7] P. J. F. White, B. W. Podaima, and M. R. Friesen, "Algorithms for smartphone and tablet image analysis for healthcare applications," *IEEE Access*, vol. 2, pp. 831–840, Aug. 2014.

[8] C. Kratzke and C. Cox, "Smartphone technology and apps: Rapidly changing health promotion," *Int. Electron. J. Health Edu.*, vol. 15, pp. 72–82, 2012.

[9] D. L. Berry *et al.*, "Enhancing patient-provider communication with the electronic self-report assessment for cancer: A randomized trial," *J. Clin. Oncol.*, vol. 29, no. 8, pp. 1029–1035, Mar. 2011.

[10] A. Samad, S. Hayes, and L. French, "Digital imaging versus conventional contact tracing for the objective measurement of venous leg ulcers," *J. Wound Care*, vol. 11, no. 4, pp. 137–140, 2002.

[11] S. M. Rajbhandari *et al.*, "Digital imaging: An accurate and easy method of measuring foot ulcers," *Diabetic Med.*, vol. 16, no. 4, pp. 339–342, Apr. 1999.

[12] M. L. Hill, R. C. Cronkite, D. T. Ota, E. C. Yao, and B. J. Kiratli, "Validation of home telehealth for pressure ulcer assessment: A study in patients with spinal cord injury," *J. Telemed. Telecare*, vol. 15, no. 4, pp. 196–202, 2009.

[13] *Multi Measures; TapeMeasure!* [Online]. Available: https://play.google.com, accessed Dec. 20, 2014.

[14] *SmartMeasure; Ruler*. [Online]. Available: https://itunes.apple.com, accessed Dec. 18, 2014.

[15] *Robot Electronics*. [Online]. Available: http://www.robot-electronics.co.uk/products/sensors/ultrasonics.html, accessed Oct. 7, 2015.

[16] *Robot Electronics*. [Online]. Available: http://www.robot-electronics.co.uk/products/sensors/infrared-range.html, accessed Oct. 7, 2015.

[17] Lytro. *You'll Never Think About Pictures the Same Way*. [Online]. Available: https://www.lytro.com/camera, accessed Oct. 7, 2015.

[18] (Dec. 27, 2012). *Toshiba Putting Focus on Taking Misfocusing Out of Photos*. [Online]. Available: http://ajw.asahi.com/article/economy/business/AJ201212270054, accessed Feb. 25, 2014.

[19] S. Dent. (Oct. 22, 2013). *Nokia's Refocus Lens Camera App Promises Infinite Depth of Field Control*. [Online]. Available: http://www.engadget.com/2013/10/22/nokias-refocus-lens-camera-app/, accessed Feb. 24, 2014.

[20] S. Pinto. (Feb. 27, 2014). *Dual-Lens Smartphone Camera: Killer Feature or Just a Gimmick?* [Online]. Available: http://www.techtree.com/content/news/5615/dual-lens-Smartphone-camera-killer-feature-gimick.html, accessed Feb. 27, 2014.

[21] C. Rother, R. Kolmogorov, and A. Blake. *GrabCut Interactive Foreground Extraction Using Iterated Graph Cuts*, Microsoft Research, Cambridge, U.K. [Online]. Available: http://cvg.ethz.ch/teaching/cvl/2012/grabcut-siggraph04.pdf, accessed Jul. 16, 2015.

[22] P. Foltynski, P. Ladyzynski, and J. M. Wojcicki, "A new smartphone-based method for wound area measurement," *Artif. Organs*, vol. 38, no. 4, pp. 346–352, Apr. 2014.
[23] Z. Zhang, "A flexible new technique for camera calibration," *IEEE Trans. Pattern Anal. Mach. Intell.*, vol. 22, no. 11, pp. 1330–1334, Nov. 2000. [Online]. Available: http://research.microsoft.com/en-us/um/people/zhang/Papers/TR98-71.pdf, accessed Oct. 30, 2014.
[24] R. Y. Tsai, "A versatile camera calibration technique for high-accuracy 3D machine vision metrology using off-the-shelf TV cameras and lenses," *IEEE J. Robot. Autom.*, vol. 3, no. 4, pp. 323–344, Aug. 1987.
[25] J. Anderson and J. Baltes, "A pragmatic global vision system for educational robotics," in *Proc. AAAI Spring Symp., Semantic Sci. Knowl. Integr.*, 2007, pp. 1–6. [Online]. Available: http://www.aaai.org/Papers/Symposia/Spring/2007/SS-07-09/SS07-09-001.pdf, accessed Jul. 18, 2015.
[26] *NPUAP Pressure Ulcer Stages/Categories*. [Online]. Available: http://www.npuap.org/resources/educational-and-clinical-resources/npuap-pressure-ulcer-stagescategories/, accessed Aug. 24, 2014.

TIK WAI (KIRAL) POON received the B.Sc. degree in computer engineering from the University of Manitoba, in 2014, where he is currently pursuing the degree in computer science. He has participated on the University of Manitoba's team in several international robotics competitions and the Canadian Satellite Design Challenge. He was active in the local IEEE Student Chapter (UMIEEE) from 2010 to 2013, including serving on its executive committee. He is currently a member of the IEEE Winnipeg Section Education Chapter.

MARCIA R. FRIESEN received the Ph.D. degree in biosystems engineering from the University of Manitoba, Winnipeg, MB, Canada, in 2009. She is currently a Multidisciplinary Engineering Researcher with active research in engineering education and computer modeling and simulation. She is an Associate Professor of Design Engineering with the University of Manitoba. She was the President of the Association of Professional Engineers and Geoscientists of Manitoba.